Isolating transits from molecular dynamics data with application to the equation of state

Duane C. Wallace, Sven P. Rudin, and Giulia De Lorenzi-Venneri
Theoretical Division, Los Alamos National Laboratory, Los Alamos, New Mexico 87545, USA

(Received 28 July 2020; accepted 12 October 2020; published 2 November 2020)

In vibration-transit theory of liquid dynamics, the atomic motion consists of two contributions: First-principles vibrational motion in a $3N$-dimensional liquid potential energy valley, plus transits, which operate to move the atoms between valleys. In one time step, when an atom crosses the intersection between two valleys, moving a very small distance, the atom's equilibrium position moves the very large distance between the equilibrium positions of two neighboring valleys. A figure showing this simultaneous two-part motion is presented early in this paper. We recognize the motion of the equilibrium position as the transit motion, and we verify that this motion can be observed and measured. We present a collection of single-atom transit-motion profile graphs extracted from molecular dynamics liquid trajectories. These graphs confirm that vibrations plus transit motions constitute nearly the entire liquid atomic motion. While the transit motion is never fully resolved on the liquid trajectory, it is by definition fully resolved on the trajectory of equilibrium positions. The transit contribution to thermodynamics is calibrated via two adjustable parameters in the transit partition function. The transit contribution to the liquid thermal energy is graphed and discussed. The condensed-matter atomic motion theory of thermodynamic functions for crystals and liquids is outlined with particular attention to recent developments in the equation-of-state program.

DOI: 10.1103/PhysRevB.102.184301

I. INTRODUCTION

Vibration-transit (VT) theory of liquid dynamics is being developed primarily for equilibrium thermodynamic functions, for equation-of-state (EOS) applications. The theory has reached the stage where the foundational principles are determined, and fixed, and theory accounts for experimental and molecular dynamics (MD) data to very good accuracy. It is now an appropriate time to present the theory in detail, to clarify its unique points of view, and to provide some guidelines for application. To this end, we planned a series of three research reports to cover the three major components of the theory, to be followed by comparisons of theory with experiment and MD. The first two reports are published, and are briefly summarized in the following two paragraphs, on topics relevant to the transit research that follows here.

The long-standing lore of many-body theory is that the potential energy surface (PES) for an N-atom condensed-matter system consists of an enormous number of $3N$-dimensional intersecting potential energy valleys. Our first VT theory report, a large-scale quench study of Na at the volume of the liquid at melt, V_m^l, not only verified this lore but added valuable theoretical information about the potential energy distributions of the major condensed-matter phases [1]. The structures lie in two distributions: The lower-lying *symmetric* distribution, composed of a wide spread of amorphous solids, with the stable bcc Na at the bottom, plus the highest-lying distribution of *random* structures, narrowly spread and of overwhelming numerical superiority. Moreover, the potential energy of the liquid structure, i.e., a representative random structure, is recognized as the liquid ground-state energy in classical statistical mechanics. In quantum theory, the vibrational zero-point motion is also included in the ground state. Many additional informative notes are recorded in this report.

In the second VT report, the vibrational theory for one (any) random potential energy valley is constructed [2]. It is shown how the vibrational frequencies are calculated, how they calibrate the Hamiltonian, and how the resulting thermodynamic functions are calculated in quantum and classical statistical mechanics. In addition to these operational procedures, the theoretical concepts underlying the application of vibrational theory to the liquid state are presented in detail. It cannot be overemphasized that the entire vibrational theory is calculated from a single random valley taken from the actual liquid potential energy surface. The vibrational thermodynamic functions are therefore from first principles, meaning no adjustable parameters; every application of this vibrational theory is 100% predictive. Finally, the vibrational contribution to liquid thermodynamics is the dominant contribution, which places the complications all in the small transit contribution. This construction is classic many-body theory, and it provides highly accurate statistical mechanical results for the liquid from a knowledge of just the major physical properties of transits.

We now turn to transit theory, the subject of this report. In the early years of VT theory, the emphasis was on the calculation of transit contributions to thermodynamic functions. This program has been remarkably successful in accounting for the internal energy and entropy of elemental liquids at the melting temperature T_m, and to high T; a summary is provided in Sec. II of [1]. Transit theory was consolidated in an approximate configuration integral, and the corresponding formulas

for transit thermodynamics were derived [3]. That work has since been updated, and we were preparing the update for the third VT theory report when a breakthrough came on another front, and changed our priorities.

The only pictures we have of actual transits are from MD trajectories of Na and Ar at temperatures of 30.0 and 17.1 K, respectively [4]. The graphs show Cartesian components of single-atom trajectories versus time t. All the transits show a common motion: A segment of vibration about a constant equilibrium position, then a permanent displacement of the equilibrium position, then a continuation of the vibration about the new equilibrium position. In passing, we note that the MD systems studied here, Na and Ar, are indeed liquids in the transit pictures, because they are moving among random valleys, which constitute the liquid domain; however, they are frozen, and metastable.

Some time later, when we looked for transits in liquid Na at 395 K, a bit above melting, they were not to be seen. This started a long investigation into what was going on. In time, we reached the conclusion that changed everything: To see transits at $T \gtrsim T_m$, we shall have to separate the pure vibrational motion from the motion of the equilibrium positions.

In Sec. II, a procedure is established to extract one-atom transits from MD data, and it is applied to our MD system for liquid Na at 395 K. Through a set of figures with their detailed discussions, the character of single-atom transit motion is illustrated. In Sec. III, a well-developed definition of the transit motion is assembled from a variety of technical perspectives. In Sec. IV, a brief update is presented for our original partition-function formulation of transit thermodynamics [3]. In Sec. V, the relevance of VT theory to recent advances in EOS construction technique for crystal and liquid phases is discussed.

II. RESOLVING TRANSITS

To isolate the motions of the equilibrium positions, we create a "quench trajectory," as follows. From the liquid trajectory, the MD system is quenched to its underlying N-atom equilibrium configuration at every time step. We work with $N = 500$. The quench trajectory consists of the set of equilibrium positions $\boldsymbol{R}_K(t_n)$, for atom K with $K = 1, 2, \ldots, N$, at time steps t_n with $n = 0, 1, \ldots$. It is necessary to verify that this trajectory belongs to the liquid phase, not to an amorphous solid; this issue is discussed in Sec. IV of [1].

In analyzing the quench trajectory, one must keep in mind that it does not express atomic motion, but it does express the motion of the atomic equilibrium positions. Precisely this point is what enables the quench trajectory to resolve transits. An illustrative drawing is presented in Fig. 1. Qualitatively, when a liquid atom K crosses an intervalley intersection, it moves an ordinary small distance $|\delta \boldsymbol{r}_K|$ on the liquid trajectory. At the same time, the quench trajectory measures the much larger distance $|\delta \boldsymbol{R}_K|$ between the atom's initial and final equilibrium positions. In more detail, Fig. 1 is based on a simple mean-atom approximation for the vibrational motion. The atom moves in a three-dimensional spherically symmetric harmonic well centered on its equilibrium position; its mean probability density is a spherical surface, which is projected as a circle in Fig. 1. This part of the description is the

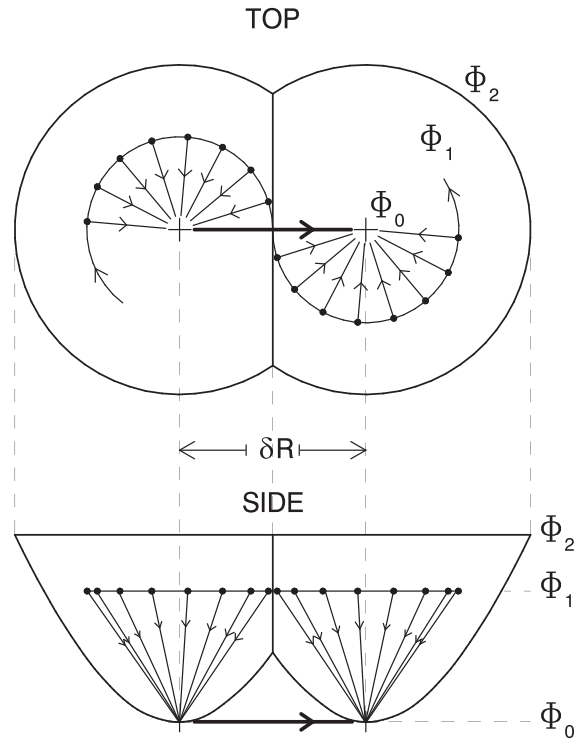

FIG. 1. How a single transit is revealed by the quench trajectory. Top and side projections of the potential surface of two intersecting valleys, truncated above, are shown by the enclosing outer lines and the central intersection lines. The two continuous circular lines show the trajectory of one atom moving above the potential surface. The two potential minima are marked with plus signs, and the arrows pointing to the minima show a sequence of quenches of the atom from its trajectory to a minimum. The transit is the motion of the equilibrium position from the initial to the final minimum, left to right on the horizontal line, of distance δR, occurring when the atom passes above the intersection. The potential energies are Φ_0 at the minima, Φ_1 on the atomic trajectory, and Φ_2 on the PES truncation.

beginning of the construction of a transit configuration integral, to be installed in the VT partition function. Such a simplified picture is satisfactory for transit theory, since ultimately it will be calibrated from MD or experimental data.

Our primary instrument for analyzing the quench trajectory is the distance graph, $d_K(t_n)$ versus t_n, where

$$d_K(t_n) = |\boldsymbol{R}_K(t_n) - \boldsymbol{R}_K(t_0)|. \tag{1}$$

t_0 is the start time of a distance graph, and t_0 can be chosen arbitrarily on the quench trajectory. An important point is that $d_K(t_n)$ is not a time correlation function. $d_K(t_n)$ *does* measure a correlation, but it is not averaged over atoms K, nor over start times t_0. While a time correlation function carries out these averages, and returns a sequence of mean values, $d_K(t_n)$ presents a single-atom measure of distance versus time. This level of precision is possible only by evaluating $d_K(t_n)$ on the quench trajectory instead of the liquid trajectory. To be sure, the graphs are noisy, but the physical processes are clear enough, and that is the information we seek.

We begin by making a quench trajectory long enough for a good supply of transits, and by making distance graphs for all N atoms in the MD system, from different start times t_0

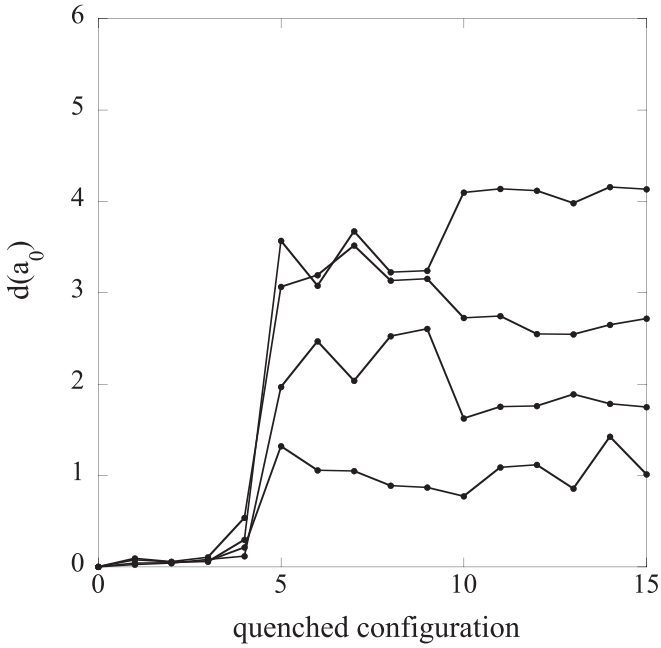

FIG. 2. Four distance graphs showing intervalley transits on the time step $t_4 - t_5$. The distance is measured from the equilibrium position at t_0 [see Eq. (1)]. Up to t_4 the distance is very small, and generally can be approximated by zero, while after t_5 the distance is well approximated by a horizontal line at the mean value, plus standard deviation.

if needed. To isolate each single transit in a short segment of undisturbed trajectory, we study the first transit of each distance graph; the reason is given at the end of this section. In Figs. 2 and 3, the dominant distance increase in one δt of each graph is identified as the transit. The eight graphs show

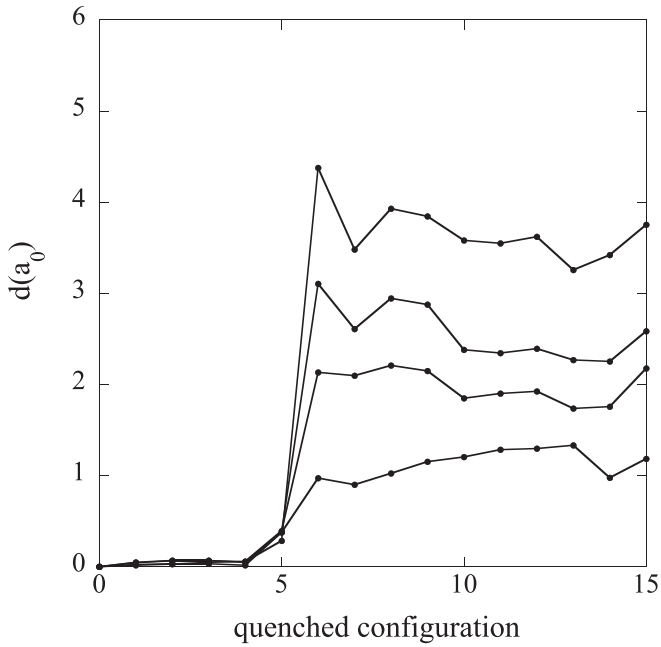

FIG. 3. Four distance graphs showing intervalley transits on the time step $t_5 - t_6$. The remaining description is the same as in Fig. 2.

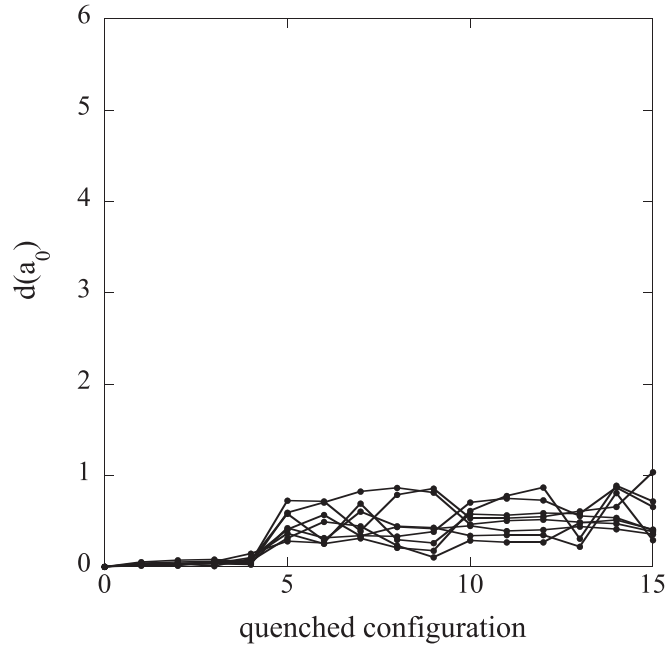

FIG. 4. Eight distance graphs showing intravalley transits on the same time step. See the discussion in the text.

a uniform behavior in three time intervals, as follows. The low-lying segment ahead of each transit shows that the atomic equilibrium position remains close to its initial equilibrium position, until the first transit appears. The high-lying segment following each transit shows that the final equilibrium position also remains constant, with moderate fluctuations. The transit itself is quite fast, proceeding essentially in a single δt. In our assessment, all three of these graphical characteristics must be visually present in order to certify that the graph constitutes a transit. Obviously, what appears in a distance graph strongly depends on the value of δt; trial and error is in order here.

In our system, a transit takes place in one time step. Over the system, the number of transits in one time step fluctuates, but our graphs are generally chosen to show a group of transits in the same time step, for visual clarity of the overall figure.

For a more incisive examination of distance graphs, we need to separate transits into two qualitative categories. An intervalley transit is one in which an atom crosses an intervalley intersection, and the atom's initial equilibrium position moves to its next one, just as shown in Fig. 1. At the same time, the equilibrium positions of nearby atoms move short distances in order to maintain a proper liquid structure. These motions are referred to as intravalley transits.

A collection of intravalley transits, appearing in the same δt as the intervalley transits of Fig. 2, is shown in Fig. 4. We have chosen to put transits of less than $1a_0$ in the intravalley category. As a result, Figs. 2 and 4 together, or Figs. 3 and 4 together, show one complete distribution, from near the highest transit distance observed, down to zero. The separation at $1a_0$ has only qualitative theoretical significance.

Figure 5 shows a collection of distance graphs in each of which an intravalley transit appears ahead of an intervalley transit. The presence of the earlier short-distance transit appears to have no effect on the character of the following

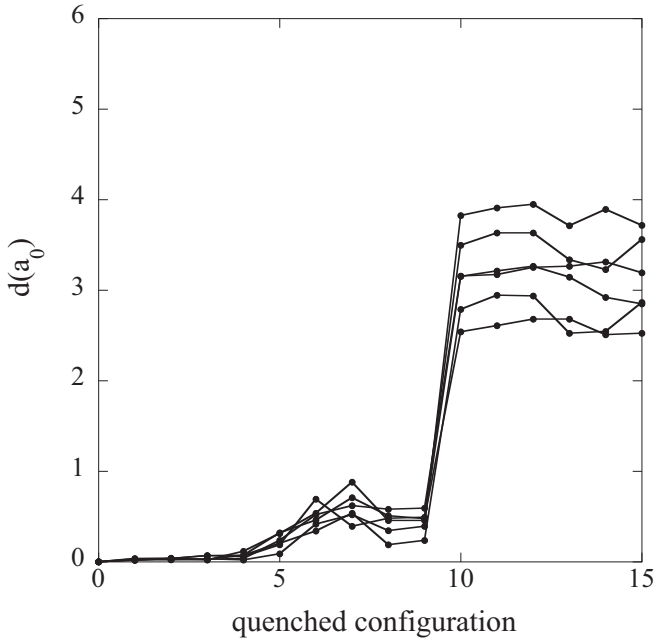

FIG. 5. Six distance graphs showing intravalley transits, each followed by an intervalley transit. See the discussion in the text.

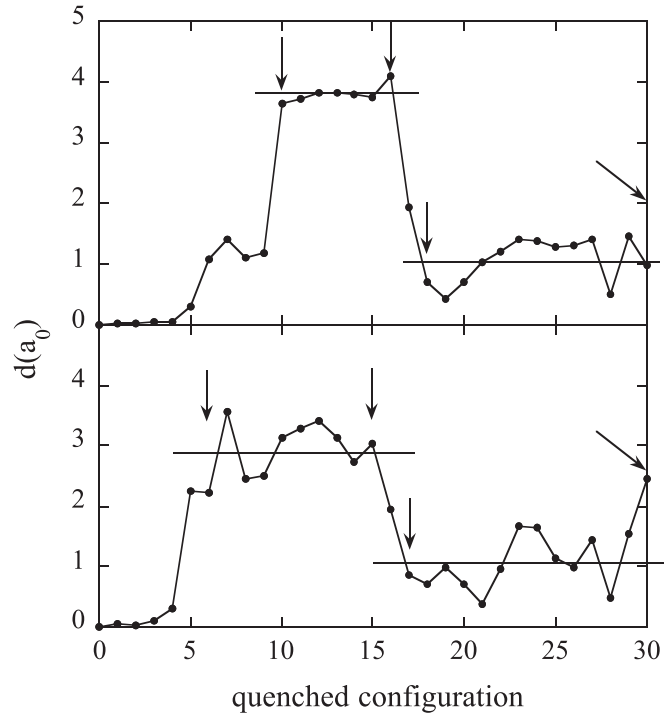

FIG. 6. Two transit return graphs, in which a transit returns to near its starting distance. To bring out the underlying graph character, approximately constant segments are replaced by mean-segment horizontal lines. The arrows encompass the set of dots averaged in one line. In the top graph, the horizontal lines emphasize the characteristic transit-return shape. In the bottom graph, the horizontal lines eliminate an oppressive level of noise.

intervalley transit. But that appearance cannot be substantiated in Fig. 5. Each atom shows two successive distances, both measured from a common initial position at t_0, but at an unknown intersection angle. To see the effective interaction between transits, we need to see the graphs in three dimensions.

In our estimation, the intravalley transits are almost certainly fluctuations. Their origin is as follows. Each liquid structure has very strong global correlations, produced by the constraint of zero force on every atom, together with the periodic boundary conditions. At $T \gtrsim T_m$, all motions of the equilibrium positions are proceeding in a steady state, and sampling different configurations, which have significant variations in their structural correlations. This produces system-wide fluctuations in the distance graph of every atom. At t_0, the system is in a single global structure, and some time is required to build up the fluctuations as $t_n - t_0$ increases. This is the tentative cause of the larger fluctuations after the transit than before it.

The complete theoretical motion is then described by three contributions: Vibrational motion of the atoms about fixed equilibrium positions $\boldsymbol{R}_K(t_0)$, plus the motion of the equilibrium positions $\boldsymbol{R}_K(t_n) - \boldsymbol{R}_K(t_0)$ due to intervalley transits, plus ordinary fluctuations about the equilibrium positions $\boldsymbol{R}_K(t_0)$, due to intravalley transits over the entire system. Then VT theory is changed only by the addition of a fluctuation, normally negligible as a finite-N effect. And the fluctuation contributes nothing to self-diffusion. Figure 4 supports this view, since the mean value of the distance remains constant after the first intravalley transit operates. On the other hand, Fig. 5 is unable to inform us on this issue.

Occasionally in a distance graph, sometime after the first transit, $d_K(t_n)$ decreases again to nearly where the transit began. The motion is called a "transit return," or simply "return." Two graphs are shown in Fig. 6. Partial returns also appear. The returns are not useful in studying single transits, but on rare occasions they do show an interesting two-point repetition where a transit cannot make up its mind on which valley to take.

One more significant motional effect appears in the distance graphs, and that is an overlay of scatter in varying degree. The curves in Figs. 2–5 show scatter at a normal level; Fig. 7 shows a wider variation. In general, the type of motion appearing in a distance graph can be seen through the scatter.

As a final discussion of this section, we shall propose an operational control that will remove uncertainties in the interpretation of distance graphs. The control is the "First-of-the-First Transit Rule," and it applies when one wants to study single transits of single atoms. There are two parts.

(a) *Problem*: As observed in Figs. 2–4, we can interpret the first transit, but we cannot interpret the second transit in Fig. 5. *Solution*: In any distance graph, the initial and final equilibrium segments must be in place, and only the first transit is kept for study.

(b) *Problem*: As transits proceed, the atomic equilibrium positions begin to drift away from their positions at t_0. *Solution*: In any distance graph, keep transits appearing only in an early time interval, say until around 10% of the system atoms have transited.

Our ultimate transit analysis follows the preceding two rules. Distance graphs were constructed for the 500 atoms

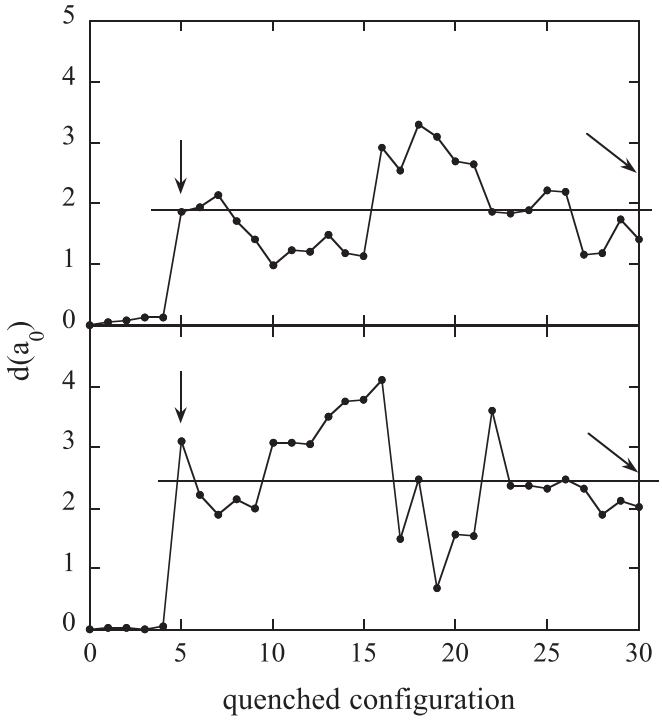

FIG. 7. Two very noisy distance graphs, converted to useful intervalley transits by averaging out the noise. The horizontal fitted line transforms a segment of variable data into a single accurately measured data point. The transit distance δR is the distance from the point at t_4 up to the horizontal line.

in our system, and were examined by eye. Approximately half of these graphs exhibited the required stationary segment before and after the transit. Of these acceptable graphs, approximately 60% were single transits like the ones shown in Figs. 2–4 and 7. Another 30% were return transits like the one shown in Fig. 6. While these graphs have various levels of noise, there were an ultimate 10% of graphs so noisy that they could not be interpreted. This overall collection of graphs is rather constant in our studies of one system at a single temperature. The liquid system studied here is based on an interatomic pair potential with a long successful history for crystal and liquid sodium.

III. DEFINING TRANSITS

We can now say that transits in the liquid at $T \approx T_m$ are real. They have been extracted from MD data.

From scanning the behavior of many distance graphs, it is clear that the graphs presented here express the dominant character of the motion of the atomic equilibrium positions in the liquid at T around T_m. From the information presented in Sec. II, we are able to make a quantitative definition of transits: A single-atom transit is the motion of its equilibrium position from one potential energy minimum to another. Specifying this motion makes the definition precise, and clearly separates the vibrational and transit motions. Some years ago, we introduced the VT decomposition of the liquid atomic motion [5]: The atoms undergo vibrational motion about the equilibrium positions of a static $3N$-dimensional potential energy valley, interspersed with a steady-state macroscopic motion of the equilibrium positions. This definition is still correct, but now the second word "motion" can be replaced by "transit motion."

The present transits carry their own unique information, at the microscopic level. Transits observed here are at the single-atom level, hence they are the characteristic input data for many-body theory. However, the present transits are seen only in two dimensions. Eventually, they need to be studied in three dimensions. This will not be difficult now that transits are readily extracted from MD data. Ultimately, by bringing transits into three dimensions, they could in principle be assembled with the $3N$-dimensional vibrational motion to create a characteristic atomic-level motion of liquid dynamics.

From the introduction of the name *transits* in liquid dynamics theory, we have identified it with the motion of atomic equilibrium positions [last topic in Sec. VI of [5]; Sec. II D of [6]; text below Fig. 3 of [7]; Eq. (9) and following text of [8]]. In the $3N$-dimensional potential energy surface, an atom moves from one valley to another by crossing the intervalley intersection. Occasionally we have referred to this crossing as a transit, because with the crossing the atom's equilibrium position moves from one valley to another. However, this second usage differs noticeably from the first, and we shall remove it from our lexicon.

It is now clear why we could not find transits on the liquid trajectory at $T \gtrsim T_m$. The transit motion appears in one δt in Fig. 1, and in the distance graphs of Sec. II. On the liquid trajectory, after a transit, an atom moves over its new potential energy surface, remaining distant from the equilibrium position, as shown in Fig. 1. The liquid trajectory incorporates the transit motion in approximately the time it takes for the atom to move once around its circle in Fig. 1. That time is measured in the mean-square displacement as $60\delta t$ (see Table 1 and figures showing τ_{RW} in [7]); so the liquid trajectory is very slow to incorporate the transit motion, too slow for visual resolution of the transit. We can remove this problem entirely only by working with the quench trajectory.

Two well-known historical markers pointed the direction to where we are today. Almost a century ago, Frenkel [9,10] argued that the motion of a liquid atom consists of approximately harmonic oscillations about an equilibrium point, while the equilibrium point itself jumps from time to time. Half a century later, Stillinger and Weber [11,12] suggested that the equilibrium properties of liquids result from vibrational excitations within, and shifting equilibria between, the inherent structures. However, the road to the present was not a straight line. To arrive where we are today, it was necessary to uncover the first-principles $3N$-dimensional vibrational theory that had always belonged to the liquid, and combine it with experimental data to isolate, and then define, the remaining (transit) motion. The nontrivial "isolate and define" process is shown in Fig. 1.

IV. TRANSITS AND THE EOS

Here we present a brief update on transit thermodynamics theory. This is intended to fill the gap in our three-part series on advances in VT theory, created when we chose to make the present report about transits observed in the liquid at $T \gtrsim T_m$.

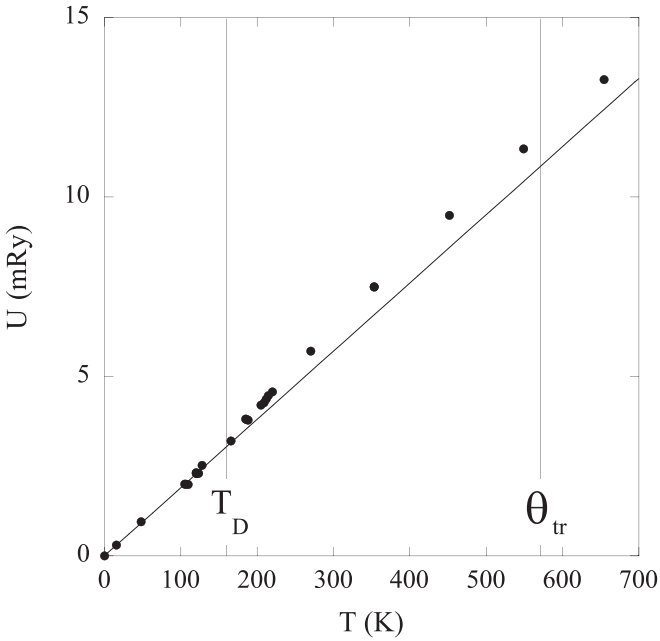

FIG. 8. The internal energy measured from Φ_0^l vs T. Dots are $U_{\rm MD}(T)$, heavy line is $3k_BT$, and $\Phi_{\rm tr}(T)$ is dots minus line, according to Eq. (4). $\Phi_{\rm tr}(T)$ is zero up to the start of self-diffusion at $T_D \approx 160$ K, is maximum at the transit scaling temperature $\theta_{\rm tr} = 570$ K, and curves downward and goes negative at T around 1100 K (see Fig. 1 of [2]).

The transits discussed in this section are the mean transits formulated from a configuration integral [3], and in terms of which all transit thermodynamic functions are constructed. The newly observed transits described in Secs. II and III are presumably the raw material for the transits discussed here.

We shall work in classical statistical mechanics, at the fixed volume V_m^l. The internal energies from VT theory and MD, respectively, are $U_{\rm VT}(T)$ and $U_{\rm MD}(T)$. The VT theory equation is

$$U_{\rm VT}(T) = \Phi_0^l + U_{\rm vib}(T) + \Phi_{\rm tr}(T), \tag{2}$$

where Φ_0^l is the structural potential energy, $U_{\rm vib}(T)$ is the vibrational internal energy, and $\Phi_{\rm tr}(T)$ is the transit contribution, and is pure potential energy. To apply Eq. (2) to the EOS, it is necessary to calibrate the terms on the right side.

At $T = 0$, Φ_0^l is the only nonzero term on the right side of Eq. (2), in classical statistical mechanics. Notes on the calibration of Φ_0^l in DFT calculations are provided in Appendix B of [13] and the supplemental material of [14]. It is important that Φ_0^l is taken from the potential energy valley that is given to the Hamiltonian (see paragraph 1 of Sec. III of [2]).

The vibrational potential surface is the entire liquid potential energy up to the level where transits appear in the atomic motion. Also, $U_{\rm vib}(T)$ is $3k_BT$ at all T. Therefore, the system internal energy is

$$U_{\rm VT}(T) = \Phi_0^l + 3k_BT \tag{3}$$

for T up to where transits contribute significantly to the potential energy. This behavior is numerically verified in Fig. 8, where $U_{\rm VT}(T)$ and $U_{\rm MD}(T)$ are graphed versus T: $U_{\rm MD}(T)$ stays with $3k_BT$ to around 160 K.

Upon increasing T from zero, two transit properties become observable at the common temperature $T_D \approx 160$ K. The transit energy $\Phi_{\rm tr}(T)$ and self-diffusion coefficient $D(T)$ both increase from zero at T_D [see Fig. 10 of [15] for the $D(T)$ graph]. By definition, the vibrational motion has no diffusive component. We conclude that transits are entirely responsible for self-diffusion.

At $T > T_D$, $U_{\rm VT}(T)$ is given by Eq. (2). To evaluate $\Phi_{\rm tr}(T)$ from Eq. (2), we set $U_{\rm VT}(T) = U_{\rm MD}(T)$. Equation (2) then becomes

$$\Phi_{\rm tr}(T) = U_{\rm MD}(T) - \Phi_0^l - 3k_BT. \tag{4}$$

Figure 8 shows the calibration of $\Phi_{\rm tr}(T)$, directly from $U_{\rm MD}(T)$.

Our first calibration procedure was developed to simultaneously calibrate 13 elemental liquids, whose $\Phi_{\rm tr}(T)$ follow a common temperature-scaling behavior [3]. This $\Phi_{\rm tr}(T)$ is calibrated with two element-specific parameters, namely the scaling temperature $\theta_{\rm tr}$ and the transit potential energy ϵ. We have developed a simpler but much more flexible procedure to calibrate one liquid at a time, without reference to scaling, but with the same calibration parameters. This procedure employs Eq. (4) to evaluate $\Phi_{\rm tr}(T)$.

The last step is to calibrate and test Eq. (4) as follows. As the two parameters are varied, the error on the right side of Eq. (4), i.e., the error in $U_{\rm MD}(T) - \Phi_0^l$, can be mapped. The map can be used to find the best fit to $U_{\rm MD}(T)$ over any chosen range of temperature, to the liquid phase boundary and beyond. Moreover, the map will give notice of where the theory begins to fail, and will assist in finding the cause. Finally, since we have thermodynamic consistency over the complete VT formulation, any pair of calibrated parameters $\theta_{\rm tr}$ and ϵ can be tested simultaneously for additional thermodynamic functions, e.g., the entropy and so on.

When the calibration of $\Phi_{\rm tr}(T)$ is accomplished, we have Eq. (2) for the liquid energy $U_{\rm VT}(T)$, where in Fig. 8 $U_{\rm vib}(T)$ is the line at $3k_BT$, and adding $\Phi_{\rm tr}(T)$ produces a very good fit of $U_{\rm VT}(T)$ to the dots. Thermodynamic consistency then certifies an accurate curve for the specific heat $C_V(T)$ as well. Figure 8 also shows the key character of VT theory wherein the vibrational energy dominates the total energy, while the transit contribution is only around 10% of the total. This construction is classic many-body theory, with the major contribution being first principles and tractable, and the complicated contribution being small and subject to continued research. Further discussion of VT thermodynamics may be found in [3,5,13,14]. We are currently working through VT theory at increasing temperatures, accounting for thermodynamic functions as far as we can, to where theory falls below the MD data and the system enters the liquid-to-gas regime.

V. VT THEORY AND THE EOS

Our intention in this last section is to briefly compare two theoretical procedures for the calculation of thermodynamic functions, the procedure from many-body theory on the one hand, and that from EOS research on the other. Our primary concern here is the low-temperature phases, crystals and the liquid. The many-body theory of atomic motion in a crystal, and the corresponding statistical mechanical formulation of

thermodynamic functions, is known as lattice dynamics. This theory is first principles, based entirely on the vibrational potential energy surface of the crystal. Just as in the crystal, the liquid also has a $3N$-dimensional harmonic potential energy surface rising from the minima of the liquid structure. In VT theory, the liquid atomic motion is again first principles, based on the vibrational surface, plus transits, which move the atoms among potential surface equilibrium positions.

The EOS cold curve is the lattice-dynamics structure potential energy of the lowest-lying crystal at $T = 0$ as a function of compression (see the early work of [16]). In the last several years, EOS research has investigated the application of lattice-dynamic phonon densities of state (DOSs) to the EOS construction [17–20]. All these calculations are first principles. The temperature dependence of the phonon data is generally negligible, because crystals exist at low temperatures. On the other hand, the large volume variations required in EOS applications provide a computational challenge to the phonon DOS calculations. For each crystal at each volume, the information in one phonon DOS graph encodes the vibrational contributions to all thermodynamic functions at all temperatures. The authors were able to conclude that their EOS applications are treated within the lattice-dynamic framework [19].

For the liquid phase, the situation is quite different from the crystal phases. Allowing a rather broad generalization, there is a commonly used procedure, and perhaps the most well-tested one, for the liquid EOS. That is to employ a Mie-Grüneisen EOS in the vicinity of the liquid-crystal interface, and interpolate it with appropriate modifications all the way to the ideal gas. This liquid-phase model is employed beyond the crystal-phase studies mentioned above [17–19]. An analytic Mie-Grüneisen EOS has also been constructed for the same application [21]. An old parametrized interpolation model running from crystal to ideal gas is also in common usage [20]. The temperature range spanned by these models is very large, and covers the major behaviors of liquid, gas, and ideal gas. We shall return to this point of departure shortly below.

The phonon theory of liquid dynamics is being developed from a different point of view (for a review, see [22]). The thermal energy is attributed to a Debye distribution of frequencies [23], and self-diffusion is accounted for by a modification of the lowest-frequency transverse modes [24–26]. A recent formulation for all temperatures includes solid, liquid, and gas phases, and culminates in a classical hard-sphere system representing the ideal gas [27]. With the present transit study, together with the results of current work on liquid thermodynamics, a detailed comparison of VT theory and the phonon theory becomes appropriate, and will be included in our next research report.

Our ultimate conclusion follows. The crystal EOS can be calculated from lattice dynamics in first principles. The higher-lying liquid EOS is generally calculated from a Mie-Grüneisen formulation. As temperature increases from T_m, the atoms move increasingly above intervalley intersections, and the vibrational motion disintegrates. There is no phase change here, but disappearance of the liquid state is observable and has to be accounted for as temperature continues to increase. This is accomplished through a slowly operating modification of the Mie-Grüneisen EOS. Further modifications will be required to carry the system to the ideal gas. Now, however, a new paradigm is available, or soon shall be. With VT theory, one can add a second well-defined first-principles liquid phase to the EOS foundation of crystal phases. In our present liquid Na system, liquid theory is accurate for temperatures to around $8T_m$. The condensed-matter crystal-plus-liquid EOS will therefore be accurate for temperatures to around $8T_m$ before having to start the Mie-Grüneisen EOS. This will limit the demands on that EOS. This should also allow an increase in accuracy, because the disintegration of the liquid vibrational motion is explicitly accounted for by transits.

ACKNOWLEDGMENTS

The authors would like to thank Scott Crockett for helping with the references to EOS work, Dana Delia Simionescu for helping with the figures, and Lorenzo Venneri for his contribution to the analysis of the quench trajectories. This work was supported by the US DOE through Contract No. 89233218NCA000001.

[1] T. Sjostrom, G. DeLorenzi-Venneri, and D. C. Wallace, Phys. Rev. B **98**, 054201 (2018).
[2] D. C. Wallace, S. Rudin, G. DeLorenzi-Venneri, and T. Sjostrom, Phys. Rev. B **99**, 104204 (2019).
[3] D. C. Wallace, E. D. Chisolm, N. Bock, and G. De Lorenzi-Venneri, Phys. Rev. E **81**, 041201 (2010).
[4] D. C. Wallace, E. D. Chisolm, and B. E. Clements, Phys. Rev. E **64**, 011205 (2001).
[5] D. C. Wallace, Phys. Rev. E **56**, 4179 (1997).
[6] G. De Lorenzi-Venneri, E. D. Chisolm, and D. C. Wallace, Phys. Rev. E **78**, 041205 (2008).
[7] D. C. Wallace, G. De Lorenzi-Venneri, and E. D. Chisolm, J. Phys.: Condens. Matter **28**, 185101 (2016).
[8] D. C. Wallace, E. D. Chisolm, and G. De Lorenzi-Venneri, J. Phys.: Condens. Matter **29**, 055101 (2017).
[9] J. Frenkel, Z. Phys. **35**, 652 (1926).
[10] J. Frenkel, *Kinetic Theory of Liquids* (Clarendon, Oxford, 1946), Chap. III, Sec. 1.
[11] F. H. Stillinger and T. A. Weber, Phys. Rev. A **25**, 978 (1982).
[12] F. H. Stillinger and T. A. Weber, J. Chem. Phys. **80**, 4434 (1984).
[13] N. Bock, E. Holmström, T. B. Peery, R. Lizárraga, E. D. Chisolm, G. De Lorenzi-Venneri, and D. C. Wallace, Phys. Rev. B **82**, 144101 (2010).
[14] S. P. Rudin, N. Bock, and D. C. Wallace, Phys. Rev. B **90**, 174109 (2014).
[15] D. C. Wallace and B. E. Clements, Phys. Rev. E **59**, 2942 (1999).
[16] J. M. Wills, O. Eriksson, and A. M. Boring, Phys. Rev. Lett. **67**, 2215 (1991).

[17] A. A. Correa, L. X. Benedict, D. A. Young, E. Schwegler, and S. A. Bonev, Phys. Rev. B **78**, 024101 (2008).
[18] L. X. Benedict, T. Ogitsu, A. Trave, C. J. Wu, P. A. Sterne, and E. Schwegler, Phys. Rev. B **79**, 064106 (2009).
[19] L. X. Benedict, K. P. Driver, S. Hamel, B. Militzer, T. Qi, A. A. Correa, A. Saul, and E. Schwegler, Phys. Rev. B **89**, 224109 (2014).
[20] T. Sjostrom, S. Crockett, and S. Rudin, Phys. Rev. B **94**, 144101 (2016).
[21] P. F. Weck, K. R. Cochrane, S. Root, J. M. D. Lane, L. Shulenburger, J. H. Carpenter, T. Sjostrom, T. R. Mattsson, and T. J. Vogler, Phys. Rev. B **97**, 125106 (2018).
[22] K. Trachenko and V. V. Brazhkin, Rep. Prog. Phys. **79**, 016502 (2016).
[23] K. Trachenko, Phys. Rev. B **78**, 104201 (2008).
[24] K. Trachenko and V. V. Brazhkin, Ann. Phys. **347**, 92 (2014).
[25] C. Yang, M. T. Dove, V. V. Brazhkin, and K. Trachenko, Phys. Rev. Lett. **118**, 215502 (2017).
[26] Y. Fomin, V. Ryzhov, E. N. Tsiok, J. Proctor, C. Prescher, V. Prakapenka, K. Trachenko, and V. V. Brazhkin, J. Phys.: Condens. Matter **30**, 134003 (2018).
[27] D. Bolmatov, D. Zav'yalov, M. Zhenenkov, E. T. Musaev, and Y. Q. Cai, Ann. Phys. **363**, 221 (2015).